

# Determination of Mean Velocity and Discharge in Natural Streams Using Neuro-Fuzzy and Neural Network Approaches

Onur Genç · Özgür Kişi · Mehmet Ardıçoğlu

Received: 17 December 2013 / Accepted: 21 February 2014  
© Springer Science+Business Media Dordrecht 2014

**Abstract** The applicability of artificial neural networks (ANNs) and the adaptive neuro-fuzzy inference system (ANFIS) for determination of mean velocity and discharge of natural streams is investigated. The 2,184 field data obtained from four different sites on the Sarımsaklı and Sosun streams in central Turkey were used in the study. ANNs and ANFIS models use the inputs, water surface velocity and water surface slope, to estimate the mean velocity and discharges of natural streams. The accuracies of both models were compared with the multiple-linear regression (MLR) model. The comparison results showed that the ANFIS model performed better than the ANNs and regression models for estimating mean velocity and discharge. The ANN model also showed better accuracy than the MLR model. The root mean square errors (RMSE) and mean absolute relative errors (MARE) of the MLR model were reduced by 88 and 91 % using the ANFIS model in estimating discharges, respectively. It is found that the optimal ANFIS model with RMSE of 0,063, MARE of 3,47 and determination coefficient ( $R^2$ ) of 0,996 in the test period is superior in estimation of discharge than the MLR model with RMSE of 0,532, MARE of 38,9 and  $R^2$  of 0,776, respectively. The study reveals that the ANFIS technique can be successfully used for estimating the mean velocity and discharge of natural streams by using only the inputs of water surface velocity and water surface slope.

**Keywords** Natural streams · Mean velocity · Discharge · ANNs · ANFIS · Linear regression

## 1 Introduction

Stream flows have many properties such as discharge, mean and maximum velocity, energy loss, shear stress distributions, turbidity and sediment discharge. Determination of mean

---

O. Genç (✉)  
Department of Civil Engineering, Melikşah University, Kayseri, Turkey  
e-mail: ogenic@melikshah.edu.tr

Ö. Kişi  
Department of Civil Engineering, Canik Başarı University, Samsun, Turkey

M. Ardıçoğlu  
Department of Civil Engineering, Erciyes University, Kayseri, Turkey

velocity and discharge over the open channel cross-section is very important with respect to water management, water supply, allocation of irrigation water, flood control projects, and the production of hydroelectric energy. The purpose for the investigation of flow properties such as shear stress, mean velocity and discharge is to reduce the risk in a decision taken at any given point of interest. Also, the development and application of an efficient water resource management usually require the analysis of flow properties data.

Although many researchers have studied hydraulics in stream flow, there are still many complex problems in the determination of flow properties. The simplifying of cross-section averaged one dimensional hydraulics equations is usually utilized to describe flows in open channels and rivers. However, generalization of these methods for all open channels which have different hydraulic conditions and geometric shape is difficult. Flow measurement methods are not very effective and extremely sensitive to roughness parameters. Measurement of velocity samples requires considerable effort and time (Ardiclioglu et al. 2012).

The velocity-area method is one of the most commonly used methods which can be used in discharge measurement. However, its utilization requires the mean slice velocity and also the cross-sectional area for measured cross-sections. Application of the velocity-area method is difficult and almost impossible to perform because of the significant floods events. Chezy, Darcy–Weisbach and Manning's equations, which are called slope-area methods, have been developed to determine discharge. These empirical equations are not very effective, are all extremely sensitive to roughness parameters and are not easy to determine (Chow 1959).

Prediction of flow properties such as discharge and mean velocity is very important when measurements are unavailable or insufficient (Pulido-Calvo and Portela 2007). For this purpose, many models have been used to forecast the properties of stream flow within recent years. Many researchers have used data-based models such as stochastic models to solve these problems. Data-based models have been improved for the forecasting of discharge of stream flow in the past decades (Marques et al. 2006). Autoregressive (AR) and autoregressive moving average (ARMA) have played an important role in river flow estimation (Salas et al. 1985; Maria et al. 2004). Artificial neural networks (ANNs) models can be used for solving such problems in river hydrodynamics. ANNs are a current model that have been successfully used in hydrological research, such as rainfall-runoff modeling, stream flow forecasting, precipitation forecasting, groundwater modeling, water quality and management modeling (ASCE 2000); (Maier and Dandy 2000).

Recently, the ANNs and adaptive neuro-fuzzy inference system (ANFIS) techniques have been successfully used in hydraulic sciences. Yang and Chang (2005) investigated the applicability of ANNs for simulating velocity profiles, velocity contours and for estimating the discharges accordingly. Chu and Chang (2009) used a neuro-fuzzy technique for modeling a dynamic groundwater remediation design. Kocabas and Ulker (2006) estimated the critical submergence for an intake in a stratified fluid media by using a neuro-fuzzy approach. Dogan et al. (2007) predicted the sediment concentration obtained by experimental study by using ANNs. Cobaner et al. (2008) used an ANN model for estimating bridge backwater. Mamak et al. (2009) successfully used ANFIS and ANN techniques for bridge afflux analysis through arched bridge constrictions. Kocabas et al. (2009) used the ANNs approach for predicting the critical submergence for an intake in a stratified fluid media. Bilhan et al. (2010) used two different neural network techniques for modeling lateral outflow over rectangular side weirs. Emiroglu et al. (2010) predicted the discharge coefficient of a triangular labyrinth side weir located on a straight channel by using ANFIS. Emiroglu et al. (2011) estimated the discharge capacity of a triangular labyrinth side-weir located on a straight channel by ANNs. Kisi et al. (2013) successfully used the ANFIS approach for estimating the discharge capacity of rectangular side weirs. Emiroglu and Kisi (2013) predicted discharge coefficient for the

trapezoidal labyrinth side weirs located on a straight channel. To the best knowledge of the authors, there is no published work related to the application of the ANFIS and ANN methods for prediction of mean velocity and discharge of natural streams. Iglesias et al. (2014) studied on turbidity prediction in river basin in Spain. They used artificial neural networks for turbidity prediction in order to lower costs in the quality assessment of water bodies.

In this paper, the applicability of the ANNs and ANFIS approaches for modeling mean velocity and discharge of streams is investigated. The results are compared with the multiple-linear regression model (MLR).

## 2 Field Measurements

Flow measurements were implemented at four different cross-sections in two different streams in central Turkey. These stations within the Kızılırmak basin are Barsama, Bünyan and Şahsenem on the Sarımsaklı Stream, which is a tributary of the Kızılırmak River (Fig. 1). The other station within the Seyhan basin, named Sosun, is on the Sosun stream, which is a tributary of the Zamantı River. Six velocity measurements were carried out for each of the Barsama, Bünyan and Şahsenem stations between 2005 and 2010. Four velocity measurements were carried out for Sosun station between 2009 and 2010. The velocity measurements were undertaken by using Acoustic Doppler Velocimeter (ADV). The ADV measures three-dimensional flow velocities ( $u$ ,  $v$ ,  $w$ ) for  $x$ ,  $y$ ,  $z$  dimensions in a sampling volume using the Doppler shift principle. During flow measurements, according to the water surface width, cross-sections were split into a number of slices. Point velocities for each vertical slice were measured in the vertical direction starting from a point that is 4 cm above the streambed. Measurements were repeated every 2 cm from this point to water surface.

The flow characteristics at each site are given in Table 1. In this table the first and second columns show visit numbers and dates,  $Q$  is the discharge calculated by velocity-area method,

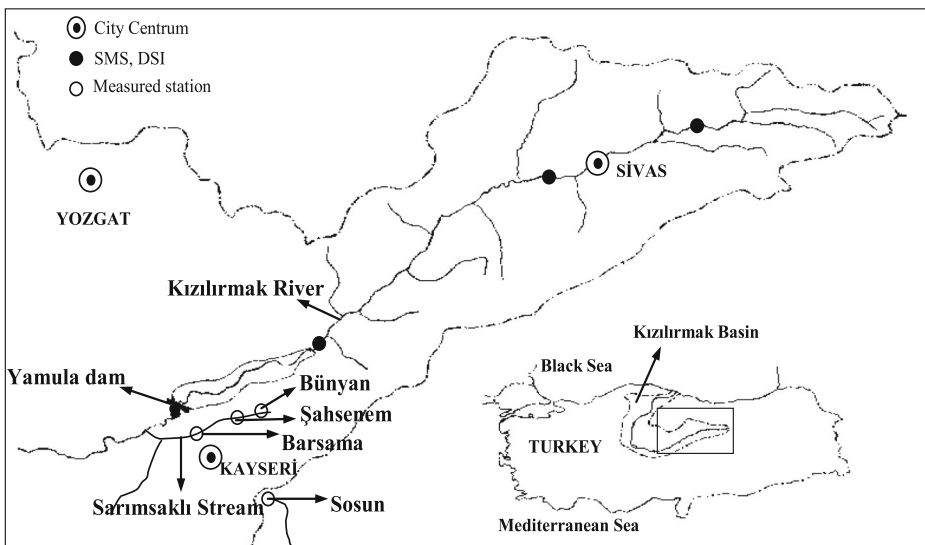


**Fig. 1** Location of the study area and measured stations, Barsama, Bünyan, Şahsenem and Sosun

**Table 1** Flow characteristics for Barsama, Bünyan, Şahsenem and Sosun stations

Stations	Date (d/m/y)	Q (m <sup>3</sup> /s)	U <sub>m</sub> (m/s)	u <sub>ws</sub> (m/s)	H <sub>max</sub> (m)	T (m)	T/R	S <sub>ws</sub>	Re (x10 <sup>6</sup> )	Fr
Barsama_1	28/05/2005	1,810	0,890	1,60	39,0	8,3	34,00	0,0091	0,76	0,481
Barsama_2	19/05/2006	2,440	1,051	1,85	40,0	9,0	35,20	0,0036	0,94	0,531
Barsama_3	19/05/2009	3,930	1,214	2,08	45,0	9,0	29,70	0,0094	1,47	0,578
Barsama_4	31/05/2009	0,970	0,590	1,14	26,0	8,4	45,40	0,0092	0,40	0,333
Barsama_5	24/03/2010	1,510	0,806	1,55	38,0	8,6	34,40	0,0097	0,61	0,417
Barsama_6	18/04/2010	2,150	0,865	1,63	38,2	8,8	22,10	0,0120	0,85	0,421
Bünyan_1	24/06/2009	0,788	0,354	0,65	72,0	4,0	7,00	0,0020	0,71	0,133
Bünyan_2	08/02/2010	0,434	0,214	0,40	66,0	4,0	7,50	0,0030	0,40	0,084
Bünyan_3	27/09/2009	0,636	0,301	0,54	72,0	3,9	8,20	0,0022	0,50	0,113
Bünyan_4	04/04/2010	1,082	0,405	0,74	85,0	4,0	7,30	0,0018	0,78	0,140
Bünyan_5	16/05/2010	1,188	0,426	0,54	86,0	4,0	7,00	0,0024	0,85	0,147
Bünyan_6	20/06/2010	0,708	0,286	0,53	79,0	3,9	7,30	0,0010	0,53	0,103
Şahsenem_1	29/03/2006	0,816	0,600	1,04	28,0	6,0	26,80	0,0059	0,47	0,350
Şahsenem_2	20/10/2007	0,718	0,529	0,93	32,0	5,4	21,90	0,0061	0,46	0,298
Şahsenem_3	22/03/2008	0,792	0,565	0,80	33,0	6,0	22,10	0,0037	0,49	0,314
Şahsenem_4	03/05/2008	0,613	0,518	1,00	32,0	5,4	25,10	0,0045	0,39	0,307
Şahsenem_5	11/10/2008	0,667	0,536	1,01	32,0	5,5	22,00	0,0046	0,44	0,303
Şahsenem_6	08/11/2008	0,732	0,516	1,00	34,0	5,6	19,60	0,0064	0,51	0,282
Sosun_1	19/05/2009	0,886	0,561	0,96	62,0	3,2	7,49	0,0032	0,84	0,227
Sosun_2	31/05/2009	0,294	0,285	0,63	43,0	3,0	9,49	0,0016	0,32	0,144
Sosun_3	24/03/2010	0,338	0,327	0,63	45,0	2,9	8,85	0,0026	0,37	0,156
Sosun_4	18/04/2010	0,529	0,541	0,93	54,0	2,3	6,53	0,0034	0,67	0,235

$U_m (=Q/A)$  is the mean velocity, where  $A$  is the area of the cross section,  $u_{ws}$  is the measured water surface velocity,  $H_{max}$  is the maximum flow depth,  $T/R$  is the aspect ratio, with  $T$  is the surface water width,  $R (=A/P)$  is the hydraulic radius,  $P$  is the wetted perimeter,  $S_{ws}$  is the water surface slope,  $Re (=4U_m R/\nu)$  is the Reynolds number, and  $\nu$  is the kinematic viscosity, and  $Fr (=U_m/(gH_{max})^{1/2})$  is the Froude number, where  $g$  is the gravitational acceleration. Froude and Reynolds numbers show that all the flow measurements were made under subcritical and turbulent flow conditions. Determining of water surface velocity,  $u_{ws}$ , is much easier than determining mean and maximum velocities in streams. Water surface velocity can be easily determined with an object that is movable on the water surface and not too heavy, such as leaves, twigs and so on.

### 3 Computation of Mean Velocity and Discharge in Stream Flow

The velocity-area method is the most commonly used method in discharge measurement (Ardiclioglu et al. 2012). While discharge is determined by the velocity area method, mean vertical velocity is also needed. For this purpose, the measured cross-section is divided into vertical slices as shown in Fig. 2. The mean vertical velocities  $U_i$ , can be calculate using Eq. (1), where  $a_i$ , is the area under the velocity distribution,

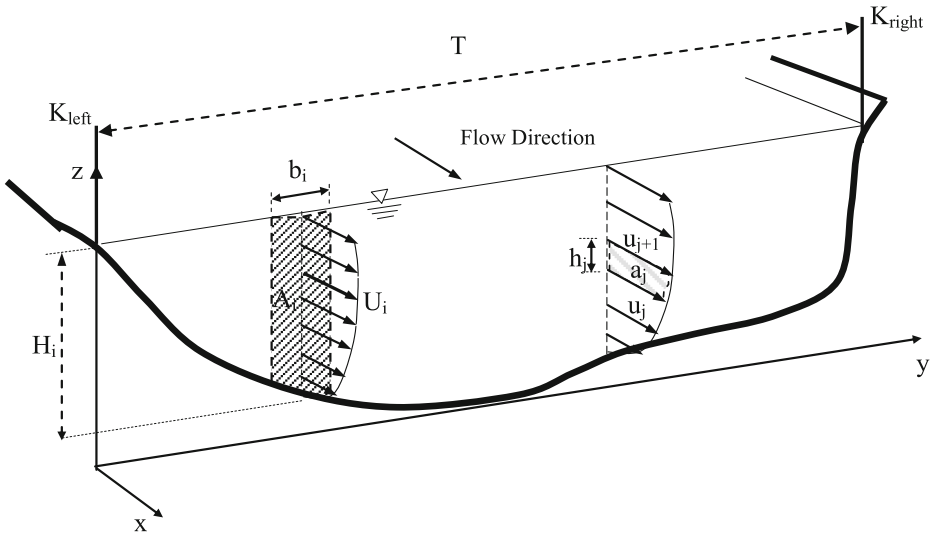


**Fig. 2** Calculation of vertical mean velocity in measured vertical

$u_{j-1}$  and  $u_j$  are the velocities and  $h_j$  is the length between two velocity measurements as shown in Fig. 2.

$$U_i = \frac{\sum a_j}{H_i} = \frac{\sum \frac{(u_j + u_{j+1})}{2} h_j}{H_i} \tag{1}$$

Slice area  $A_i$  can be calculated by Eqs. (2) and (3) is used for slice discharge where  $A_i$  is the slice area and the total flow rate of the stream is determined as the sum of the flows through all the subsections using Eq. (4). In this equation  $n$

$$A_i = b_i H_i \tag{2}$$

$$q_i = U_i A_i \tag{3}$$

$$Q = \sum_{i=1}^n q_i = \sum_{i=1}^n U_i A_i \tag{4}$$

## 4 Methods

### 4.1 Artificial Neural Networks

Artificial neural networks (ANNs) are inspired by the biological nervous system but by disregarding much of the biological detail. ANNs are massively parallel systems which consist many processing elements. The network is composed of layers comprising parallel processing elements, called neurons. Each layer is fully connected to the proceeding layer by interconnection. A three layered ANN composed of layers  $i, j,$  and  $k,$  with the interconnection weights  $W_{ij}$  and  $W_{jk}$  between layers is illustrated in Fig. 3. Initial weight values are randomly assigned and then progressively corrected during a training process. This process compares calculated

outputs to known outputs and backpropagates any errors (from right to left in Fig. 3). Thus, the appropriate weights are adjusted by minimizing the errors (Kisi 2005; Emiroglu and Kisi 2013).

Each neuron in layers  $j$  and  $k$  receives the  $x$  input which is the weighted sum of outputs from the previous layer. As an example,  $y$  for layer  $j$  is given by

$$y_{pj} = \sum_{i=1}^I W_{ij} O_{pi} + \theta_j \tag{5}$$

Where  $\theta_j$ =a bias for neuron  $j$ ,  $O_{pi}$  is the  $i_{th}$  output of the previous layer and  $W_{ij}$  is the weight between the layers  $i$  and  $j$ . An output  $f(y)$  is calculated from each neuron in layers  $j$  and  $k$  by passing its value of  $y$  through a non-linear transfer (activation) function. A commonly used transfer function is the logistic function

$$f(y) = \frac{1}{1 + e^{-y}} \tag{6}$$

Detailed theoretical information about ANNs can be found in Haykin (2009).

#### 4.2 Adaptive Neuro Fuzzy Inference System (ANFIS)

The Adaptive Neuro Fuzzy Inference System (ANFIS), which was first introduced by Jang (1993), is a universal approximator and is capable of approximating any real continuous function. ANFIS has a network structure composed of a number of nodes connected through directional links. Each node has a function which consists of fixed or adjustable parameters (Jang et al. 1997).

Assume a fuzzy inference system has three inputs ( $x, y$  and  $z$ ) and one output ( $f$ ) and the rule base contains two fuzzy IF-THEN rules of Takagi and Sugeno’s type

$$\text{RULE 1 : IF } x \text{ is } A_1, y \text{ is } B_1 \text{ and } z \text{ is } C_1 \text{ THEN } f_1 = p_1x + q_1y + r_1z + s_1 \tag{7}$$

$$\text{RULE 2 : IF } x \text{ is } A_2, y \text{ is } B_2 \text{ and } z \text{ is } C_2 \text{ THEN } f_2 = p_2x + q_2y + r_2z + s_2 \tag{8}$$

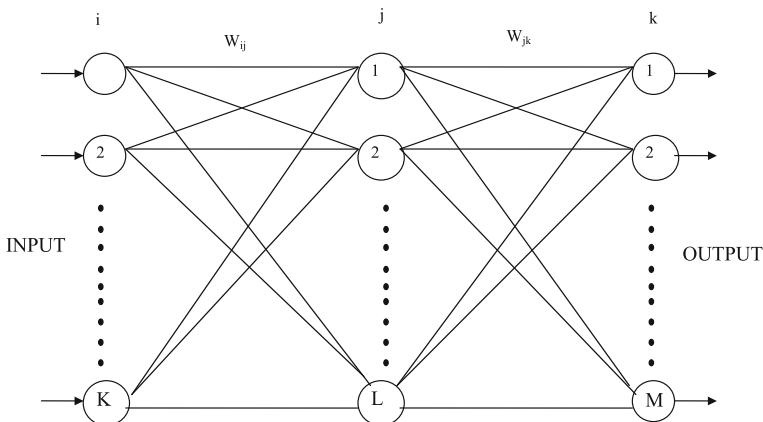


Fig. 3 A three-layer ANNs architecture (Kisi 2005)

where  $f_1$  and  $f_2$  indicate the output function of rule 1 and rule 2, respectively. The ANFIS architecture is demonstrated in Fig. 4. The node functions in each layer are summarized next.

Every node  $i$  in layer 1 has an adaptive node function

$$O_{1,i} = \varphi A_i(x), \quad \text{for } i = 1, 2, \tag{9}$$

where  $x$  is the input to the  $i_{th}$  node and  $A_i$  is a linguistic label such as “small” or “big” associated with this node function.  $O_{li}$  is the membership function of a fuzzy set  $A (= A_1, A_2, B_1, B_2, C_1, \text{ or } C_2)$ . It specifies the degree to which the given input  $x$  satisfies the quantifier  $A_i$ .  $\varphi A_i(x)$  is usually chosen to be Gaussian function with a minimum equal to 0 and maximum equal to 1

$$\varphi A_i(x) = \exp\left(-\left(\frac{x-a_i}{b_i}\right)^2\right) \tag{10}$$

where  $\{a_i, b_i\}$  are the parameters. As the values of these parameters change, the Gaussian function varies accordingly, thus exhibiting various forms of membership functions on linguistic label  $A_i$  (Jang 1993). The parameters of this layer are called premise parameters (Emiroglu and Kisi 2013).

Every node in layer 2 multiplies the incoming signals and sends the product out. For instance,

$$w_i = \varphi A_i(x)\varphi B_i(y)\varphi C_i(z), \quad i = 1, 2. \tag{11}$$

The output of each node indicates the firing strength of a rule.

In layer 3, the ratio of the  $i_{th}$  rule’s firing strength to the sum of all rules’ firing strengths is calculated by  $i_{th}$  node as

$$\bar{w}_i = \frac{w_i}{w_1 + w_2}, \quad i = 1, 2. \tag{12}$$

Every node in layer 4 has a function as

$$O_{4,i} = \bar{w}_i f_i = \bar{w}_i(p_i x + q_i y + r_i z + s_i) \tag{13}$$

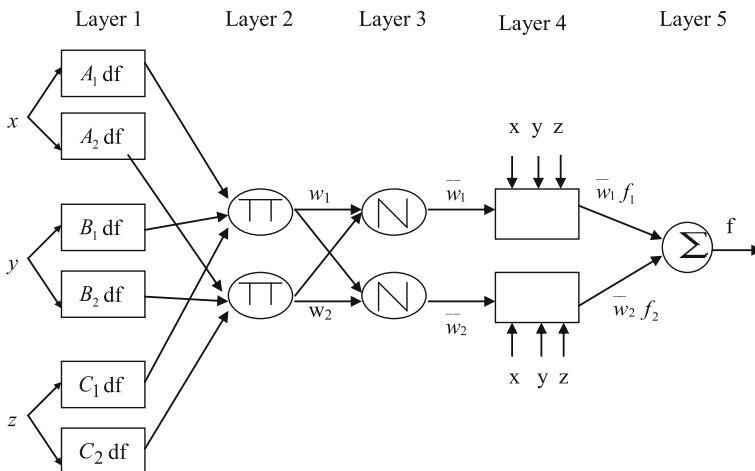


Fig. 4 ANFIS architecture (Emiroglu and Kisi 2013)

where  $\bar{w}$  is the output of layer 3, and  $\{p_i, q_i, r_i, s_i\}$  are the parameters. Each parameter of this layer is called a consequent parameter.

The single node in layer 5 computes the final output as the summation of all incoming signals

$$O_{5,i} = \sum_{i=1} \bar{w}_i f_i = \frac{\sum_i w_i f_i}{\sum_i w_i} \tag{13}$$

Thus, an ANFIS network is constructed which is functionally equivalent to a first-order Sugeno (FIS). Detailed information on ANFIS can be found in (Jang 1993).

### 4.3 Application and Results

Three different program codes were written by using MATLAB software for the ANN, ANFIS and MLR simulations. The water surface velocity  $u_{ws}$  and water surface slope  $S_{ws}$  were used as inputs to the models to estimate the mean velocity and discharges of the natural streams. For the ANN, ANFIS and regression analyses, the 2,184 measured data were used in the study. The data were randomly permuted and divided into two parts for training and testing. The first 1,747 data (80 % of the whole data) were used for training and the remaining 437 data (20 % of the whole data) were used for testing. Before applying the ANNs to the data, the training input and output values were normalized using Eq. (14)

$$c_1 \frac{x_i - x_{min}}{x_{max} - x_{min}} + c_2 \tag{14}$$

where  $x_{min}$  and  $x_{max}$  are the minimum and maximum of the training and test data. Different values can be assigned for the scaling factors of  $c_1$  and  $c_2$  because there are no fixed rules as to which standardization approach should be used in particular problems (Dawson and Wilby 1998). The  $c_1$  and  $c_2$  values were respectively taken as 0,6 and 0,2 in the present study. Thus, the input and output data were normalized between 0,2 and 0,8. The appropriate model structure was determined by using different ANN structures. The root mean square errors (RMSE), mean absolute relative errors (MARE) and determination coefficient ( $R^2$ ) statistics were used for evaluating the model accuracies. The RMSE and MARE can be expressed as

$$RMSE = \sqrt{\frac{1}{N} \sum_{i=1}^N (Y_{i,measured} - y_{i,estimate})^2} \tag{15}$$

$$MARE = \frac{1}{N} \sum_{i=1}^N \frac{|y_{i,measured} - y_{i,estimate}| \cdot 100}{y_{i,measured}} \tag{16}$$

where  $N$  is the number of the data set and  $y_i$  is the mean velocity or discharge.

Two different input combinations were used in this study for estimating the mean velocity and discharge of the natural streams. Different hidden node numbers were tried for each ANN model to determine the optimal one. The conjugate gradient algorithm (CGA) was used for



**Table 2** Training and test results of the ANN, ANFIS and MLR models in mean velocity estimation

Input	Control parameters	Training			Test		
		RMSE	MARE	R <sup>2</sup>	RMSE	MARE	R <sup>2</sup>
ANN							
$u_{ws}$	8	0,028	4,50	0,988	0,034	4,80	0,986
$u_{ws}$ and $S_{ws}$	10	0,025	4,17	0,991	0,029	4,58	0,989
ANFIS							
$u_{ws}$	(gaussmf, 7)	0,022	3,30	0,993	0,026	3,66	0,991
$u_{ws}$ and $S_{ws}$	(gaussmf, 4)	0,011	1,06	0,998	0,014	1,47	0,997
MLR							
$u_{ws}$	(0,56)	0,037	7,31	0,964	0,052	7,24	0,966
$u_{ws}$ and $S_{ws}$	(0,59–6,13)	0,035	7,19	0,967	0,050	7,04	0,968

training ANN models because CGA is more powerful and faster than the conventional gradient descent technique (Kisi 2007). The sigmoid and linear activation functions were used for the

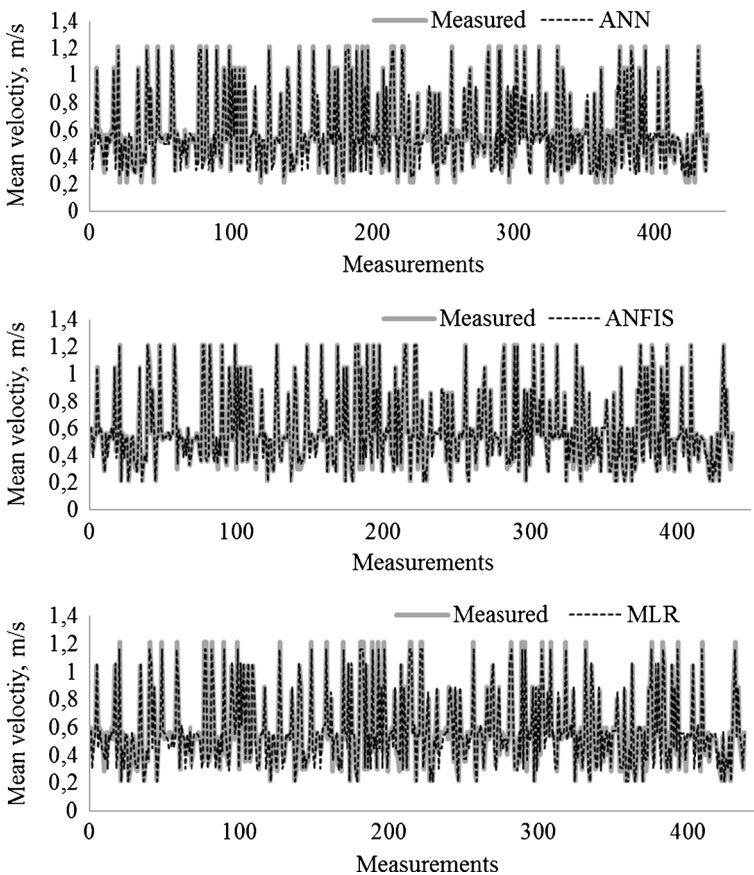


**Fig. 5** Time variation of the measured and estimated mean velocities by ANN, ANFIS and MLR models

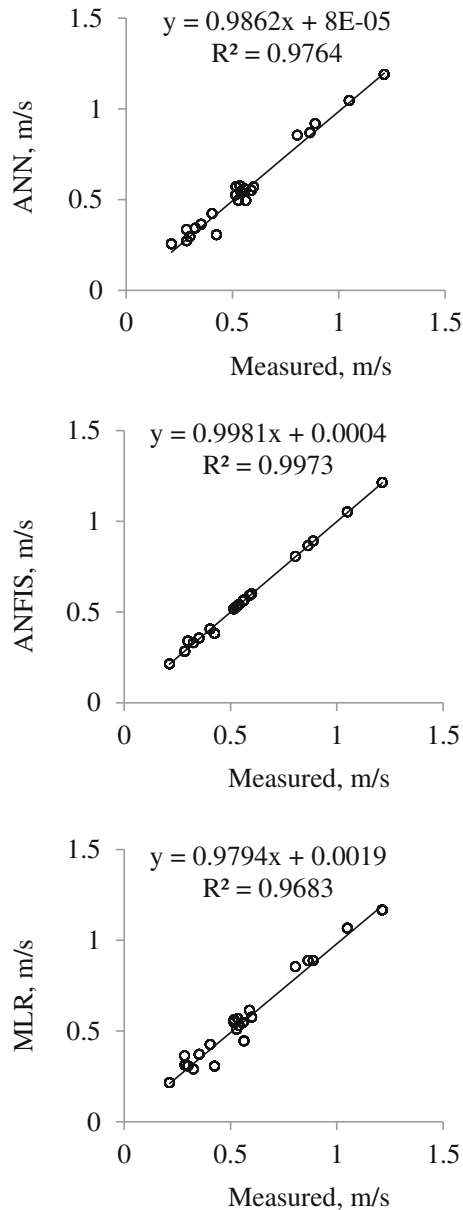


**Fig. 6** The scatterplots of the measured and estimated mean velocities by ANN, ANFIS and MLR models

hidden and output nodes, respectively. The ANN training was stopped after 1,000 epochs. The training and test results of the optimal ANNs models are given in Table 2 for estimating mean velocity. The optimal hidden node numbers are also provided in the second column of this table. It is clear from the table that the ANN model comprising inputs  $u_{ws}$  and  $S_{ws}$  performs better than the other model. To obtain the appropriate ANFIS model, different numbers of membership functions were tried. Table 2 compares the training and test performances of the

ANFIS models in mean velocity estimation. The second column of this table gives the type and optimal number of membership functions. It is clear from the table that the ANFIS model comprising four Gaussian membership functions for the inputs,  $u_{ws}$  and  $S_{ws}$  has the lowest RMSE (0,014), MARE (1,47) and the highest  $R^2$  (0,997) values in test period. The accuracy of the MLR model for each input combination is given in the last part of Table 2. The regression coefficients of the MLR models are also provided in the second column of this table. It is clearly seen from the table that the MLR model with two inputs performs slightly better than the first MLR model. A comparison of the models in Table 2 indicates that the both ANN and ANFIS models perform better than the MLR model. ANFIS model has the lowest RMSE and MARE and the highest  $R^2$  values.

Time variation of the measured and estimated the mean velocities by the ANN, ANFIS and MLR models is illustrated in Fig. 5. It is clear from the figure that the estimates of the ANFIS model are closer to the measured mean velocity values than those of the ANNs and MLR models. Underestimations are clearly seen for the MLR model. Figure 6 compares the scatterplots of the each model’s estimates in the test period. It is clear from the figure that the ANFIS has less scattered estimates than the ANN and MLR models. The MLR model seems to have the least accuracy.

The training and test results of the discharge estimates by the ANN, ANFIS and MLR models are shown in Table 3. As found for the previous application, the ANN model showed the best accuracy for the second input combination ( $u_{ws}$  and  $S_{ws}$ ). The accuracies of the ANFIS models are given in Table 3. It is clear from the table that the ANFIS model whose inputs are  $u_{ws}$  and  $S_{ws}$  has the best accuracy both in the training and test periods. Table 3 gives the training and test statistics of the discharge estimates by the MLR model. From the table, it is clear that the MLR model comprising the second input combination has the best accuracy in discharge estimation. The comparison of the models given in Table 3 clearly reveals that both the ANN and ANFIS models perform much better than the MLR model. The ANFIS model has a lower RMSE (0,063) and MARE (3,47) and the higher  $R^2$  value (0,996) than the ANN model (RMSE=0,146, MARE=14,10,  $R^2$ =0,978).

Time variation of the estimated mean discharges by the ANN, ANFIS and MLR models is compared in Fig. 7. The superiority of the ANFIS model over the ANN and especially the MLR models is clearly seen from the figures. The MLR model significantly under/over estimates measured discharge values. Figure 8 demonstrates the scatter plots for discharge estimates of each models estimate in the test period. It is clear from the figure that the estimates

**Table 3** Training and test results of the ANN, ANFIS and MLR models in discharge estimation

Input	Control parameters	Training			Test		
		RMSE	MARE	$R^2$	RMSE	MARE	$R^2$
ANN							
$u_{ws}$	1	0,207	24,6	0,944	0,218	21,4	0,95
$u_{ws}$ and $S_{ws}$	3	0,145	16,4	0,973	0,146	14,1	0,97
ANFIS							
$u_{ws}$	(gaussmf, 7)	0,123	10,4	0,980	0,142	10,9	0,97
$u_{ws}$ and $S_{ws}$	(gaussmf, 4)	0,050	2,89	0,997	0,063	3,47	0,99
MLR							
$u_{ws}$	(1,19)	0,487	44,6	0,771	0,539	40,3	0,77
$u_{ws}$ and $S_{ws}$	(1,19)	0,487	44,6	0,771	0,539	40,3	0,77

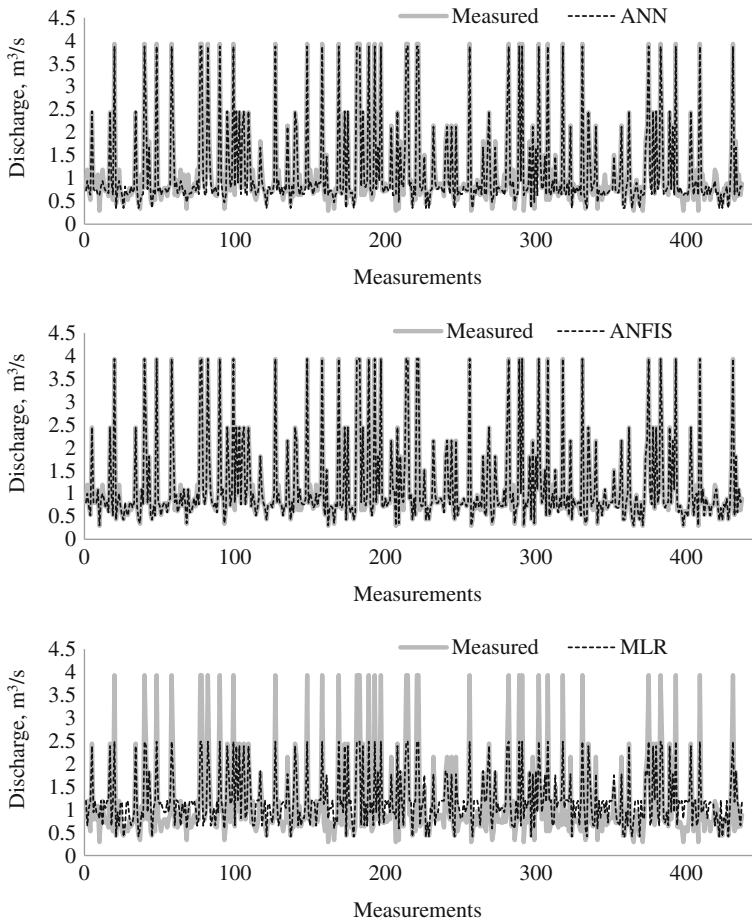


**Fig. 7** Time variation of the measured and estimated discharges by ANN, ANFIS and MLR models

of the ANFIS are less scattered and closer to the exact line (line  $45^\circ$ ) than the ANN and MLR models. The MLR model seems to be insufficient in estimating discharge.

## 5 Conclusion

The ANN and ANFIS models were developed to determine the mean velocity and discharge of streams. The 2,184 field data obtained from four different cross-sections at four sites on the Sarımsaklı and Sosun streams in central Turkey were used in this study. The water surface velocity  $u_{ws}$  and water surface slope  $S_{ws}$  were used as inputs to the models to estimate the mean velocity and discharges. After trying different numbers of hidden neurons and membership function types, the optimal ANNs and ANFIS models were obtained. The accuracy of both models was compared with those of the multiple-linear regression models. Comparison results indicated that the ANFIS model performed better than the ANNs and regression models in mean velocity and discharge estimation. Also, the ANN model was found to be better than the multiple-linear regression model. The optimal ANFIS models respectively reduced the root

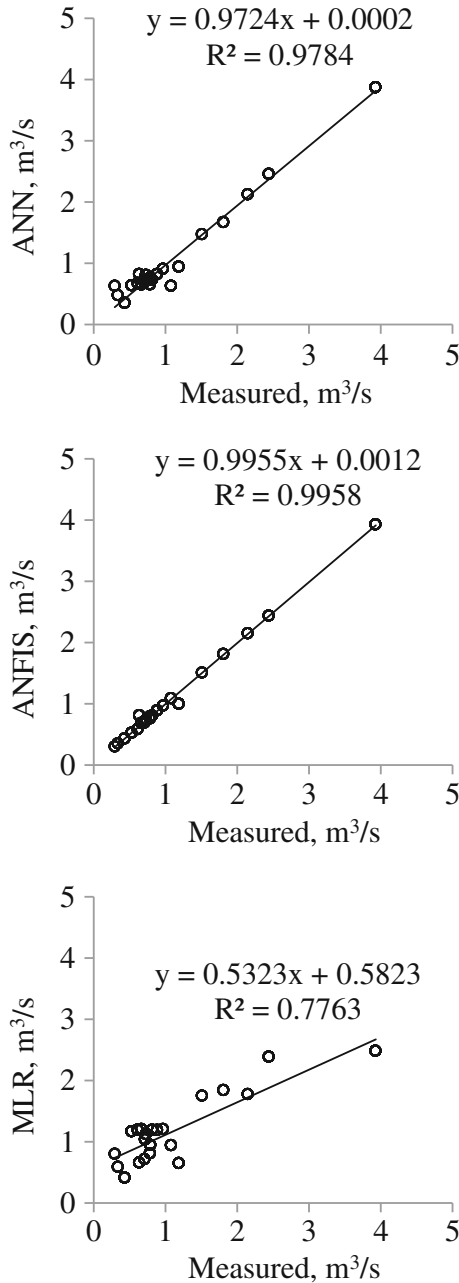


**Fig. 8** The scatterplots of the measured and estimated discharges by ANN, ANFIS and MLR models

mean square errors and mean absolute relative errors by 88 % and 91 % and increased the determination coefficient by 28 % with respect to the optimal MLR model. The study recommends that the ANFIS technique can be successfully used in estimation of the mean velocity and discharge of natural streams.

## References

- Ardiclioglu M, Genç O, Kalin L, Agiralioglu N (2012) Investigation of flow properties in natural streams using the entropy concept. *Water and Environ J*. Print ISSN 1747–6585
- ASCE Task Committee (2000) Artificial neural networks in hydrology. Preliminary concepts. *J Hydrol Eng ASCE* 5(2):115–123
- Bilhan O, Emiroglu ME, Kisi O (2010) Application of Two different neural network techniques to lateral outflow over rectangular side weirs located on a straight channel. *Adv Eng Softw* 41(6):831–837
- Chow VT (1959) *Open channel hydraulics*. McGraw—Hill Book Co., New York
- Chu HJ, Chang LC (2009) Application of optimal control and fuzzy theory for dynamic groundwater remediation design. *Water Resour Manag* 23(4):647–660
- Cobaner M, Seckin G, Kisi O (2008) Initial assessment of bridge backwater using artificial neural network approach. *Can J of Civ Eng* 35(5):500–510
- Dawson WC, Wilby R (1998) An artificial neural network approach to rainfall-runoff modeling. *Hydro Sci J* 43(1):47–66
- Dogan E, Yuksel I, Kisi O (2007) Estimation of sediment concentration obtained by experimental study using artificial neural networks. *Environ Fluid Mech* 7:271–288
- Emiroglu ME, Kisi O (2013) Prediction of discharge coefficient for trapezoidal labyrinth side weir using a neuro-fuzzy approach. *Water Resour Manag* 27(5):1473–1488
- Emiroglu ME, Kisi O, Bilhan O (2010) Predicting discharge capacity of triangular labyrinth side weir located on a straight channel by using an adaptive neuro-fuzzy technique. *Adv Eng Softw* 41(2):154–160
- Emiroglu ME, Bilhan O, Kisi O (2011) Neural networks for estimation of discharge capacity of triangular labyrinth side-weir located on a straight channel. *Expert Syst Appl* 38(1):867–874
- Haykin S (2009) *Neural networks and learning machines*, 3rd edn. Prentice Hall, New Jersey
- Iglesias C, Torres JM, Nieto PJG, Fernández JRA, Muñoz CD, Piñeiro JL, Taboada J (2014) turbidity prediction in a river basin by using artificial neural networks: a case study in northern Spain. *Water Resour Manag* 28: 319–331
- Jang JSR (1993) ANFIS: adaptive-network-based fuzzy inference system. *IEEE Trans Syst Manag Cybern* 23(3): 665–685
- Jang JSR, Sun C-T, Mizutani E (1997) *Neuro-fuzzy and soft computing: a computational approach to learning and machine intelligence*. Prentice Hall, Upper Saddle River
- Kisi O (2005) Suspended sediment estimation using neuro-fuzzy and neural network approaches. *Hydro Sci J* 50(4):683–696
- Kisi O (2007) Stream flow forecasting using different artificial neural network algorithms. *J Hydrol Eng ASCE* 12(5):532–539
- Kisi O, Bilhan O, Emiroglu ME (2013) ANFIS to estimate discharge capacity of rectangular side weir. *Water Manag* 166:479–487, WM9
- Kocabas U, Ulker S (2006) Estimation of critical submergence for an intake in a stratified fluid media by neuro-fuzzy approach. *Environ Fluid Mech* 6:489–500
- Kocabas F, Kisi O, Ardiclioglu M (2009) An artificial neural network model for prediction of critical submergence for an intake in a stratified fluid media. *Civ Eng Environ Syst* 26(4):367–375
- Maier HR, Dandy GC (2000) Neural networks for the prediction and forecasting of water resources variable: a review of modeling issues and application. *Environ Model Softw* 5:101–124
- Mamak M, Seckin G, Cobaner M, Kisi O (2009) Bridge afflux analysis through arched bridge constrictions using artificial intelligence methods. *Civ Eng Environ Syst* 26(3):279–293
- Maria CM, Wenceslao GM, Manuel FB, José MPS, Román LC (2004) Modeling of the monthly and daily behavior of the discharge of the xallas river using Box–Jenkins and neural networks methods. *J Hydrol* 296: 38–58
- Marques CAF, Ferreira J, Rocha A, Castanheira JM, Gonçalves P, Vaz N, Dias JM (2006) Singular spectral analysis and forecasting of hydrological time series. *Phys Chem Earth* 31:1172–1179
- Pulido-Calvo I, Portela MM (2007) Application of neural approaches to one-step daily flow forecasting in Portuguese watersheds. *J Hydrol* 332(1–2):1–15
- Salas JD, Tableios GQ, Bartolini P (1985) Approaches to multivariate modeling of water resources 19 time series. *Water Resour Bull* 21(4):683–708
- Yang HC, Chang FJ (2005) Modelling combined open channel flow by artificial neural networks. *Hydrol Process* 19:3747–3762